ORIGINAL ARTICLE

Expression Analysis of *miR-20a-5p*, *miR-124-3P*, *miR-125b-5p*, *Resistin*, *TLR4*, *CD36* and *TNF-α* relationship in blood mononuclear cells from patients with atherosclerosis

Maysam Mard-Soltani [1] [#] [iD], Ghazaleh Bagheri [2,3] [#] [iD], Golnar Bakhtyar [3] [iD], Fatemeh Ahmadpour [4] [iD], Arash Amin [5] [iD], Gholamreza Shahsavari [2,3]* [iD]

1. Department of Clinical Biochemistry, School of Medical Sciences, Dezful University of Medical Sciences, Dezful, Iran.
2. Cardiovascular Research Center, Shahid Rahimi Hospital, School of Medicine, Lorestan University of Medical Sciences, Khorramabad, Iran.
3. Department of Clinical Biochemistry, Lorestan University of Medical Sciences, Khorramabad, Iran.
4. Department of Clinical Laboratory Sciences, School of Allied Medicine, Lorestan University of Medical Sciences, Khorramabad, Iran, Lorestan University of Medical Sciences, Lorestan, Iran.
5. Lorestan Heart Center (Madani Hospital), Lorestan University of Medical Sciences, Khorramabad, Iran.

ARTICLE INFO

#These authors contributed equally to this work.

*Corresponding:
Gholamreza Shahsavari
Address:
Department of Clinical Biochemistry, Lorestan University of Medical Sciences, Khorramabad, Iran.
E-mail:
Shahsavari.gh@lums.ac.ir

ABSTRACT

Atherosclerosis is the primary cause of death in developed nations. The key risk factors for atherosclerosis are inflammation and lipid disorders which may all be influenced by microRNAs (miRs). This study evaluated the correlation between *miR-20a-5p, miR-124-3p, miR-125b-5p*, and key atherogenic and inflammatory genes (*TLR4, Resistin, CD36, TNF-α*) in PBMCs from patients with angiography-proven atherosclerosis. 45 healthy individuals and 45 atherosclerosis patients were selected. After sampling patients and isolating in peripheral blood mononuclear cell (PBMC) cells, gene levels were measured using real-time polymerase chain reaction. In the atherosclerosis patient group, Toll-like receptor 4 (*TLR4*) and *Resistin* were upregulated compared to the control group (p <0.05). Conversely, *miR-20a* was downregulated in patients and inversely correlated with fasting blood glucose (p <0.05). Additionally, *miR-124* expression with Resistin had a significant negative correlation (p <0.05). The study confirmed that the expression level of *miR-125b* levels may serve as a potential biomarker for atherosclerosis (p <0.01). The reduction of *miR-20a* was related to the risk of developing atherosclerosis (p <0.05). *miR-20a*, *miR-124*, and *miR-125b* present promising therapeutic targets for atherosclerosis. Since atherosclerosis has no specific clinical symptoms and early diagnosis is very important, the diagnostic biomarker *miR-125b* has the potential to significantly aid in the early detection of various diseases with an area under the curve (AUC) of 0.74, 52% sensitivity, and 74% specificity. In addition, the measurement of *miR-20a* helps determine the progression of atherosclerosis risk.

Keywords: Atherosclerosis, microRNAs, TLR4, CD36, Resistin

Introduction

In developed nations, atherosclerosis has consistently been the main cause of death. It is a vascular intima disease with internal plaques that can affect any area of the vascular system, including the aorta and coronary arteries (1-3). The first step in creating these plaques is the deposition of cholesterol crystals in the intima and smooth muscles. The fibroblasts that create connective tissue deposit calcium and cause sclerosis, or hardening of the arteries (4, 5). Chronic heart disease (CHD) occurs when atherosclerotic plaque causes narrowing of the coronary arteries, leading to stable angina. However, some plaques can rupture, leading to thrombosis, resulting in unstable angina and acute myocardial infarction (AMI) (6). Increased oxidative damage, which has an impact on lipoprotein levels, is linked to hyperlipidemia and hyperglycemia (7).

With the characterization of macrophage-derived mediators, such as cytokines, the mononuclear phagocyte function as an effector came into focus (8). The proximity of persistent atherosclerotic plaques does not necessarily lead to the occurrence of clinical events (9). It is therefore of clinical importance to rapidly identify individuals at risk for intense coronary artery disease (CAD) to prevent the morbidity and mortality that can accompany cardiovascular disease. Small, non-coding single-stranded RNAs called miRNAs (miRs) have an evolutionarily conserved size of 18 to 24 nucleotides. Genes are usually post-transcriptionally regulated by miRs binding to the 3'-UTR of target mRNA sequences, inhibiting translation and accelerating mRNA degradation, thus suppressing protein expression (10). *MiR-20a-5p* is part of the *miR-17-92* cluster (11). Research indicates that *miR-20a* significantly contributes to the development of the immune system, lungs, and heart (12).

Additionally, it has been shown to reduce inflammation by blocking the *Transforming Growth Factor* (*TGF*) signaling pathway. *MiR-20a* protects aortic endothelial cells against OX-LDL-induced inflammation by directly targeting and repressing *Toll-like receptor 4* (*TLR4*), consequently inhibiting the activation of the *nuclear factor-kappa B* (*NF-κB*) *factor* signaling pathway and the production of *tumor necrosis factor-α* (*TNF-α*) (13). *MiR-124-3p* is a conserved miRNA that plays a crucial role in various cellular functions. It is downregulated in specific

disorders such as myocardial ischaemia/reperfusion injury, stroke, and hypertension (14),(15). Forced upregulation of *miR-124* can improve LPS-associated over-secretion of *IL-1β, IL-6,* and *TNF-α (16)*. It can inhibit vascular table smooth muscle cell (VSMC) growth and counteract the stimulatory effect of ox-LDL on VSMC proliferation (17). MiR-124a controls the production of the insulin gene, and diabetic nephropathy is linked to the expression of *TNF-α*, *Resistin*, and reduction of *miR-124* in peripheral blood mononuclear cells (18). *Resistin*, a *miR-124* target (19), is increased in human monocyte-derived macrophages by oxLDL, leading to lipid accumulation and arterial inflammation. This may contribute to atherogenesis acceleration and coronary heart disease (20, 21).

Infiltration of mononuclear cells into the arterial wall and the uptake of ox-LDL, mediated by the CD36 receptor, play a pivotal role in foam cell formation. *CD36* ligands trigger a *CD36–TLR4* complex, activating *NF-κB* and increasing *TNFα* (22-24). *TNFα* promotes atherosclerosis by inhibiting cholesterol efflux, favouring cholesterol uptake by *CD36*, and downregulating *ATP-binding cassette proteins (ABCA).* which can be therapeutic in disorders like atherosclerosis and thrombosis (25). Overexpression of *miR-125b-5p* in mouse macrophages reduces *scavenger receptor B1* (*SCARB1*) expression and protein *SR-B1*, inhibiting α-HDL-mediated macrophages and decreasing cholesterol discharge, including in vascular smooth muscle cells (26). The *miR-125b* gene is located on chromosome 11q24. *MiR-125b-5p* is the dominant form of *miR-125* family that is most prevalent (27).

In an experimental model, *miR-125b* has been linked to the advancement of atherosclerosis and has been proven to be amplified in atherosclerotic plaques from the abdominal aorta of deceased patients (28). Our study indicates that the increase of miR-125b in atherosclerosis may be associated with lipid metabolism (29). As we have previously reported (29), the PBMC miR-125b was significantly higher.

We selected this specific panel of miRNAs and genes based on their established individual roles: *miR-20a, TLR4*, and *TNF-α* in endothelial inflammation; *miR-124* and *Resistin* in metabolic inflammation and insulin resistance; *miR-125b* and *CD36* in lipid metabolism and foam cell formation. Given the established roles of *miR-20a*, *miR-124*, and *miR-125b* in regulating lipid metabolism, inflammation, and

endothelial function, we hypothesized that their dysregulation in peripheral blood mononuclear cell (PBMC) would be associated with the expression of key atherogenic genes (*TLR4*, *Resistin*, *CD36, TNF-α*) in patients with atherosclerosis. Therefore, this study aimed to evaluate these relationships and assess the potential of these miRNAs as diagnostic biomarkers for AS.

Methods

Selection of study subjects

This cross-sectional case-control study examined 90 cardiology patients at the Shahid Madani Hospital who underwent angiography. The patients were divided into healthy and diseased groups with atherosclerotic lesions. 45 patients with specific lesions were considered the case group, while 45 were healthy controls, excluding those without a specific angiographic lesion. The inclusion criteria were patients with coronary angiography diagnostic (in defining the AS group, we considered the presence of calcification in the coronary arteries and included patients with a luminal narrowing percentage exceeding 20%), or therapeutic indication, while 45 individuals with completely normal angiograms (0% stenosis) were considered the healthy control group, matched age and sex, and excluded those with congenital heart disease, chronic kidney disease, pulmonary obstruction, or malignancy.

Upon admission to the angiography clinic, after informed written consent, a questionnaire containing demographic data, body mass index (BMI), age, and blood pressure was recorded. Also, a history of disease, heart attack, smoking, alcohol consumption, and exercise were recorded. Fasting blood glucose (FBS) and lipid profiles were measured for patients, and then atherogenic indices were calculated. Gensini scoring is based on a cumulative criterion in which multiple factors, such as lesion position and severity, are effective. AHA is a system of the American Heart Association. The Gensini score was calculated by multiplying a severity coefficient (1 for 1-25% narrowing, 2 for 26-50%, 4 for 51-75%, 8 for 76-90%, 16 for 91-99%, 32 for 100%) for each stenotic lesion by a multiplier based on the anatomic location of the lesion (e.g., 5 for the left main coronary artery, 2.5 for the proximal LAD, etc.). The scores for all lesions were summed to yield the total score. Unstable angina was determined based on clinical symptoms and objective evidence obtained from angiography, reflecting the presence of severe and progressive coronary artery disease. The study was approved by the Lorestan and Dezful University of Medical Sciences and the Ethics Committee at Shahid Madani Hospital in Khorramabad, Iran (IR.DUMS.REC.1398.017).

Atherogenic Indices Calculation

The atherogenic indices were calculated using formulas such as AIP (atherogenic index of plasma) = Log (serum triglyceride/serum HDLc); CRI-I (Castelli risk indices I) = serum total cholesterol/serum HDLc; CRI-II (Castelli risk indices II) = serum LDL cholesterol/serum HDLc; and TYG (Triglycerides-Glucose) = Ln ((TG×FBS)/2).

Sampling and PBMC isolation

Peripheral blood samples were collected after an overnight fast, immediately prior to the elective angiography procedure, to avoid any acute inflammatory effects of the procedure itself. Detailed information on current medication was recorded. The majority of patients in the AS group were on standard cardiovascular pharmacotherapy, including statins, antiplatelet agents, and antihypertensive drugs. There was no significant difference in medication use between the control and AS groups ($p > 0.05$), as most patients were taking statins and other medications were used much less frequently.

The study involved collecting 10 ml of blood from volunteers' peripheral veins during fasting, centrifuging 3 ml to separate serum and evaluate FBS, and isolating PBMCs using the Ficoll-Paque density gradient method (Pharmacia, Freiburg, Germany) from 7 ml of blood. The process involved pouring 3.5 ml of Ficoll into a centrifugation tube, pipetting anticoagulated blood samples over a Ficoll-Paque gradient, centrifuging at 800 g for 15 minutes, washing cells twice with PBS, and freezing isolated PBMCs for RNA isolation. The cells were then used for further analysis.

RNA extraction, cDNA synthesis, and real-time polymerase chain reaction (PCR) analysis

After being stored, cells can be recovered in a pellet by centrifuging them at 1500 g for 3 min at 4°C. RNA was extracted from the PBMC in accordance with the manufacturer's guidelines for the RNA isolation kit

(Anacell, IRAN). RNA quality was verified by obtaining A260/280 ratios between 1.9 and 2.1 for all samples. This RNA is suitable as a substrate in a variety of reactions, e.g., cDNA synthesis of mRNA and miR. The amount of total RNA was calculated using a NanoDrop 2000c spectrophotometer (Thermo Fisher Scientific) at 260 nm. Visualization of the 18S and 28S rRNA bands on electrophoresis served as a proof of RNA integrity. For cDNA synthesis, 1 µg of total RNA was used. Reverse-transcribed first-strand complementary DNA was generated using oligo-dT (Yakta Tajhiz Azma) or stem-loop (Zist Pooyesh) based gene-specific miRNA primers according to the kit method.

The benefit of using an oligo-dT primer is that cDNA synthesis begins at the intersection of the poly-A tail and mRNA. The addition of this site significantly improved detection sensitivity in other experimental systems. A real-time PCR instrument (IDEXX, Westbrook, ME, USA) was used to perform polymerase chain reaction PCR amplification and analysis. Real Q Plus 2 Master Mix Green High RO (Amplicon, Odense, Denmark) was used with specific primers for target genes (*Resistin*, *TLR4*, *TNFα*, *miR-20a*, *miR-124* and *miR-125b*), *glyceraldehyde-3-phosphate dehydrogenase* (*GAPDH*), and *SNORD-48* as internal controls. RNA sequences from GenBank were used to design primers for human mRNA via NCBI primer blast software (Table 1).

MicroRNAs and *SNORD-48* primer sequences were obtained from the Primer Assay Kit (Zist Pooyesh). The calculated annealing temperature for each set of primers was 60 C. Primers were ordered from Sinacolon (IRAN). The reaction mixture contained 20 µl of PCR mixture, and it was made as follows: 1 µl DNA, 10 µl of SYBR Green qPCR Master Mix, 1 µl of each primer, and up to 20 µl of distilled water

Table 1. Primers sequences

Name	Forward	Reverse	NM	Product Size
TNF-α	GGGACCTCTCTCTAATCAGCC	AGGGTTTGCTACAACATGGG	NM_000594.4	95
Resistin	TACTTGCCCCCGAGGCTT	CTCCGGTCCAGTCCATGC	NM_020415.4	119
TLR4	TTAATCCCCTGAGGCATTTAGGC	GAGAGGTGGCTTAGGCTCTG	NM_138554.5	127
CD36	GCAACAAACATCACCACACCA	CTTTGGCTTAATGAGACTGGGAC	NM_001001548.3	135
GAPDH	GGTCGGAGTCAACGGATTTGG	TGATGACAAGCTTCCCGTTCT	NM_002046.7	194

The Fast Start polymerase was activated and cDNA was denatured by a pre-incubation for 15 min at 95 °C; the template was amplified for 40 cycles of denaturation for 15 s at 95 °C, annealing and extension of primers at 60°C programmed for 30 s, and one step (55-95°C) for 30 min to assess the melting curve. After amplification, the Real-Time PCR products were separated using electrophoresis on a 2% polyacrylamide gel. The gel was run in a 1% Tris-borate EDTA (TBE) buffer, and electrophoresis was conducted at a constant voltage for 40 minutes. The PCR products were visualized using a UV transilluminator and compared to 50 bp DNA markers to confirm size and specificity. The data were normalized relative to the mRNA expression of the *GAPDH* and *SNORD-48* housekeeping genes and analyzed using the comparative threshold cycle Ct method (Ct). The stability of the reference genes *GAPDH* and *SNORD-48* was confirmed across all sample groups (AS and control) by comparing their Ct values, which showed no significant variation ($p > 0.05$), ensuring reliable normalization. The efficiency of the PCR reactions was validated using a standard curve, and all reactions had an efficiency between 90% and 110%. Melt curve analysis was performed at the end of each run to confirm the specificity of amplification, showing single peaks for all products.

Statistical analysis

A post-hoc power analysis using G*Power software indicated an achieved power of >80% for detecting significant differences in primary outcomes (e.g., *miR-125b* expression) with an effect size of 0.65 and alpha set at 0.05 for sample size detection. The obtained data were analyzed using commercially available IBM Statistical Package for the Social

Sciences (SPSS, Chicago, IL, USA) software. GraphPad Prism version 5.0a (GraphPad Software, San Diego, CA, USA) was used to create the graphs. By using the Kolmogorov-Smirnov test, the data's normal distribution was assessed. The Student's t-test for normal data was used to assess group differences involving continuous variables. The Mann-Whitney U tests were used to compare data that did not have a normal distribution.

By using logistic regression analysis, the relationship between gene expression and AS was estimated. The results were offered as the odds ratio (OR). *MiR-20a* and *miR-125 b*, *miR-124* mRNA expression in PBMCs was investigated using ROC (receiver operator characteristic) analysis, and the area under the curve (AUC) was calculated to assess their diagnostic potential for separating patients with AS from those without the disease. The significance was set at *p*<0.05.

Results

Basic characteristics of the subjects

Table 2 provides detailed information on the demographic and clinical characteristics of the patients. The baseline characteristics were well-matched in both groups. Age, sex, and BMI did not significantly differ between the atherosclerosis (AS) and control groups. However, in patients, triglycerides (*p*< 0.001), fasting blood glucose(*p*< 0.05), serum creatinine (*p* <0.05), . CRI-II (*p*< 0.01), AIP (*p* <0.01), and TYG (*p* <0.01) were significantly higher.

According to Table 3, the prevalence of diabetes, hyperlipidemia, and smoking was numerically higher in the AS group, though these differences did not reach statistical significance (*p*>0.05). The AS group shows a significantly higher prevalence of unstable angina and a higher number of diseased vessel. Diabetes: The AS group has a higher prevalence of diabetes (24.4%), hyperlipidemia (33.3%), smoking (28.8%), and hypertension (51.1%) compared to the control group (13.3%), with a higher smoking history in the AS group (28.8%). The AS group had a higher prevalence of unstable angina (75.6%) and three-vessel disease (44.5%), indicating more extensive coronary artery involvement.

The G-score, a measure of coronary artery disease severity, was significantly elevated in the AS group compared to the control group. Stenosis in the left anterior descending artery (LAD), right coronary artery (RCA), and left circumflex artery (LCX) was also significantly higher in the AS group.

Table 2. Basic characteristics of study participants between the two groups of atherosclerosis patients and healthy individuals

Parameter	Control (n=45) (Mean±SEM)	AS (n = 45) (Mean±SEM)	P-value
Age (years)	57.9 ± 2.13	61.6 ± 1.6	0.712
Height (cm)	164.4 ± 1.8	165.2 ± 3.4	0.144
Weight (Kg)	72.6 ± 2.32	76.4 ± 3.27	0.455
Body mass index (BMI) (Kg/M²)	26.63 ± 4.6	26.98 ± 5.4	0.850
Fasting glucose (mg/dL)	105.21 ± 6.94	120.26 ± 6.31	*<0.05
Cholesterol (mg/dL)	163.24 ± 10.35	166.1 ± 9.49	0.830
Triglycerides (mg/dL)	138.29 ± 10.28	166.94 ± 14.51	**<0.01
HDL-C (mg/dL)	45.2 ± 1.7	44.8 ± 3.4	0.250
LDL-C (mg/dL)	95.73 ± 7.04	99.23 ± 6.5	0.944
BUN (mg/dL)	32.6 ± 2.1	38.66 ± 2.4	0.157
Serum creatinine (mg/dL)	1.03 ± 0.075	1.2 ± 0.054	* <0.05
BUN/Cr	39.67 ± 6.89	34.83 ± 2.58	0.974
CRI-I	3.7 ± 0.22	4.06 ± 0.28	0.736
CRI-II	2.11 ± 0.128	2.41 ± 0.16	* <0.05
AIP	0.47 ± 0.031	0.52 ± 0.055	**<0.01

Parameter	Control (n=45) (Mean±SEM)	AS (n = 45) (Mean±SEM)	P-value
TYG	8.7 ± 0.35	9 ± 0.72	<0.01**
Gender (male / female)	20/25	28/17	0.057

Note: * *p* <0.05, ** *p* <0.01, *** *p* <0.001. AIP: Atherogenic index of plasma; CRI: Castelli's Risk Index. Data presented as Mean ± SEM. Group comparisons were made using independent Student's t-test for normally distributed data and Mann-Whitney U test for non-normal data.

Table 3. Cardiovascular risk factors and angiographic characteristics of groups

	Control (n=45)		AS (n = 45)		P-value
Parameter (Disease History)	**(N)**	**(%)**	**(N)**	**(%)**	
Diabetes	6	13.3	11	24.4	0.17
Hyperlipidemia	12	26.6	15	33.3	0.22
Smoking	8	17.7	13	28.8	0.18
Hypertension	23	51.1	20	41.5	0.23
Angiographic Characteristics	**(N)**	**(%)**	**(N)**	**(%)**	
Stable Angina	11	24.4	0	0	0.0001****
Unstable Angina	34	75.6	0	0	
No. of diseased vessels					
Single vessel	11	24.4	0	0	0.0001****
Two vessels	14	31.1	0	0	
Three vessels	20	44.5	0	0	
Angiographic Characteristics	**Mean ± SEM**		**Mean ± SEM**		***p*-value**
Gensini score	48.31 ± 5.3		0		0.0001****
Diseased vessels	1.24 ± 0.05		0		0.0001****
LAD stenosis	79.24 ± 7.8		0		0.0001****
RCA stenosis	50.22 ± 7.9		0		0.0001****
LCX stenosis	64.17 ± 8.9		0		0.0001****

Note: * *p* <0.05, ** *p* <0.01, *** *p* <0.001.

miR-124-3p and *miR-20a-5p* levels in PBMCs of patients with AS

To clarify the expression of miRs, the real-time-PCR assay was used. In another study we demonstrated that the PBMC *miR-125b* was significantly higher in patients than in healthy individuals ($p < 0.05$, 1.5 fold change) (29). Furthermore, compared to the control group, the AS group's PBMC showed significantly lower expression of the *miR-20a* gene ($p < 0.05$; Figure. 1). However, *miR-124* expression did not show a significant difference ($p > 0.05$, Figure.1). Our findings suggest that *miR-125b* and *miR-20a* dysregulation may play significant roles in the progression of AS.

Resistin, CD36, TLR4, and TNFα gene expression in PBMCs of patients with AS

In addition, we looked at *Resistin, CD36, TLR4,* and *TNFα* expression levels in the AS and control groups, four biomarkers linked to inflammation. According to our findings, patients had higher expression levels of *Resistin* and *TLR4* compared to the control group ($p < 0.05$; $p < 0.001$; Figure. 2). Although the AS group exhibited elevated expression levels of TNFα (fold change = 1.3) and CD36 (fold change = 1.2) compared to controls, these differences did not reach statistical significance ($p > 0.05$)."

Diagnostic potential of PBMC *miR- 125b- 5p* in AS

The ROC curve can be used to determine whether a variable may be able to serve as a disease biomarker. This curve is established based on sensitivity and specificity. The AUC of the ROC curve represents the test's ability to make a diagnosis. As shown in Figure 3, the increased expression of *miR-125b* in mononuclear blood cells indicates that the biomarker is appropriate for use in identifying patients with atherosclerosis from controls in the study population ($p < 0.01$).
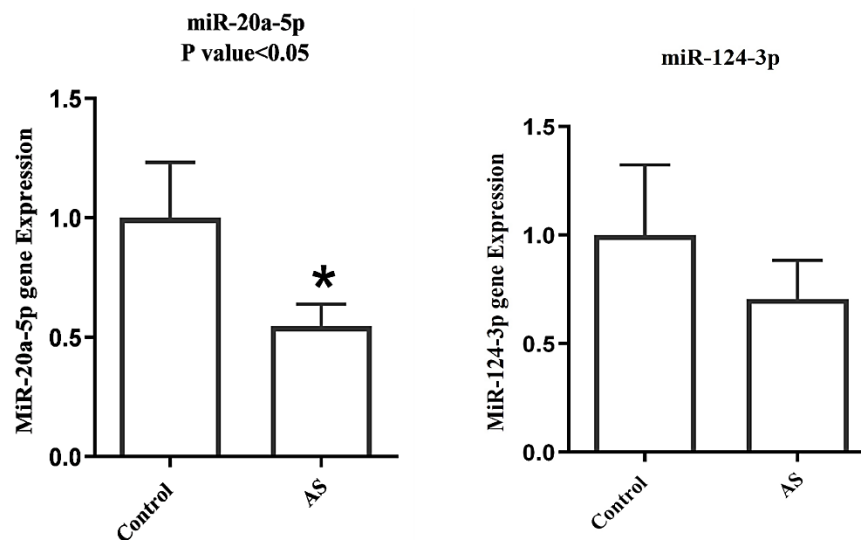

Figure 1. Expression of *miR-20a* (A, *p* <0.05) and *miR-124* (B, *p* >0.05) in PBMC cells of patients and controls. * Symbol means *p* <0.05. Relative Expression (2^−ΔΔCt) normalized to SNORD-48. Data are presented as mean ± SEM. Group comparisons were made using the Mann-Whitney U test.
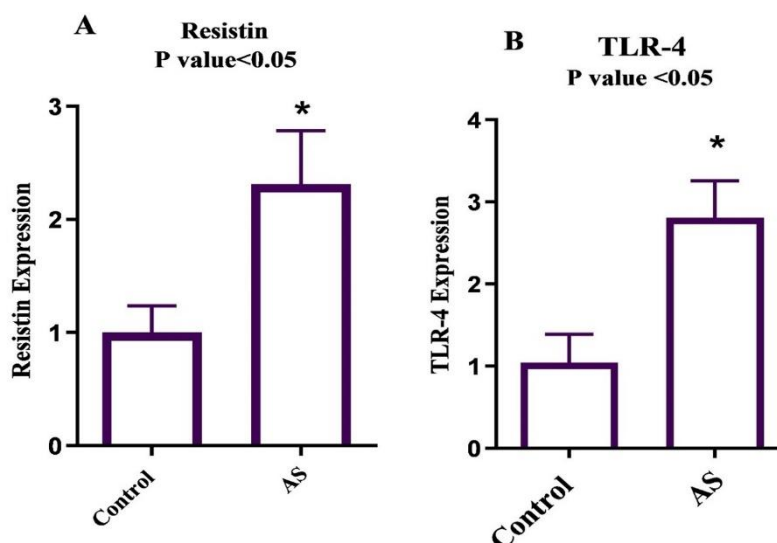

Figure 2. Expression of Resistin (A, p <0.05), TLR4 (B, p <0.05) and TNF-α (C, p >0.05) in PBMC cells of patients and controls. * Symbol means p <0.05. Relative Expression (2^−ΔΔCt) normalized to normalized to GAPDH. Data are presented as mean ± SEM. Group comparisons were made using the Mann-Whitney U test.
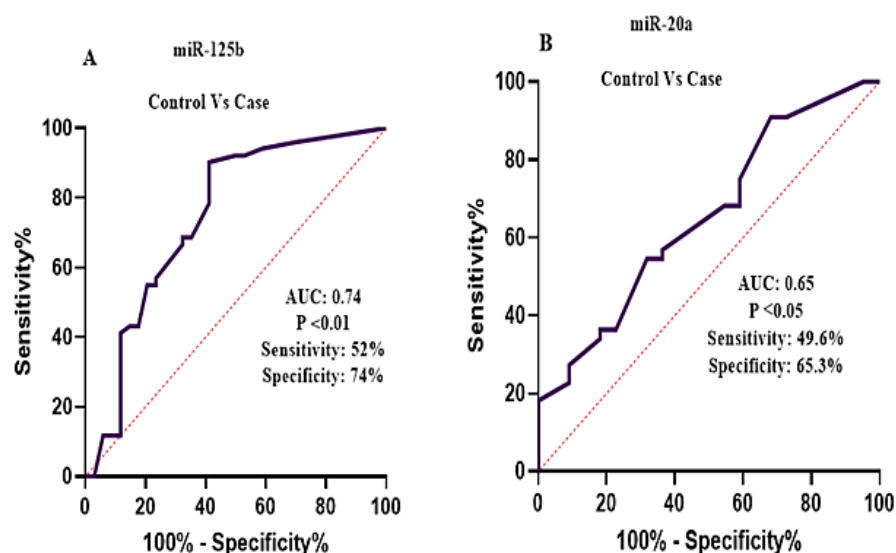
Figure 3. Receiver operating characteristic (ROC) curves for models to predict atherosclerosis. (A) AUC showed higher value in model for *miR-125b* as a new marker for AS detection (*p* <0.01). AUC = 0.74 (95% CI: 0.72-1). (B) Prediction of health groups with *miR-20a* based on ROC curve model (*p* <0.05). AUC = 0.65 (95%CI: 0.63-0.83). (*p < 0.05, **p < 0.01)."

The AUC was 0.74, the sensitivity was 52%, and the specificity was 74%. Another biomarker to distinguish patients with atherosclerosis from controls in the study population is the decreased expression of *miR-20a* in blood mononuclear cells (*p* <0.05), but the AUC was 0.65, the sensitivity was 49.6%, and the specificity was 65.3%. This suggests low discriminatory power for *miR-20a* as a standalone biomarker. As shown in Figure 4 and Table 4, ROC curve analysis based on atherosclerosis indices was used to distinguish between the control and AS groups (*miR-125b* and atherogenic indices). *miR-125b* exhibited higher values as predictor variables (AUC = 0.74, and *p*< 0.01).
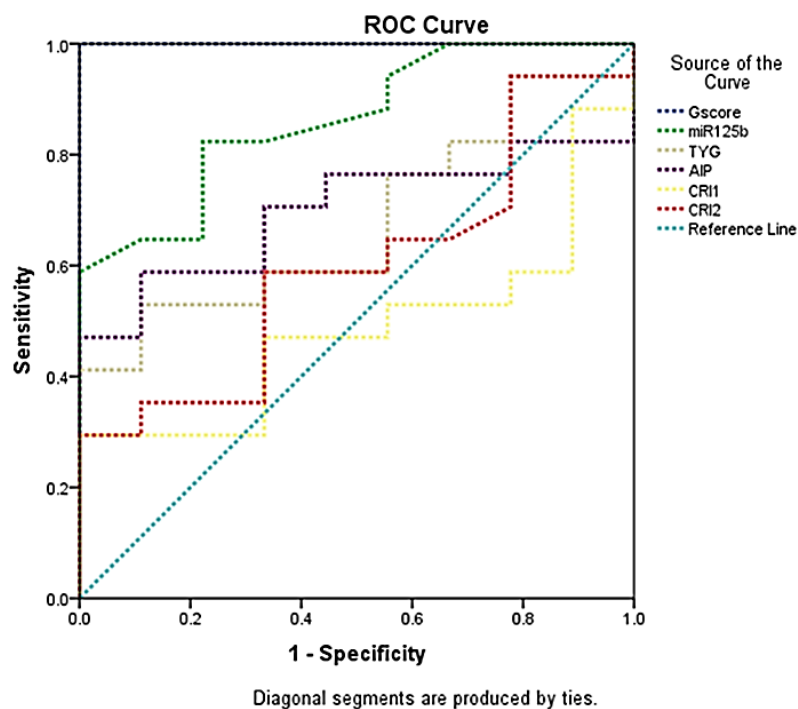

Figure 4. Receiver operating characteristic (ROC) curves for models to predict atherosclerosis. AUC showed higher value in model for miR-125b (*p* < 0.01) AUC = 0.74 (95% CI: 0.72-1). Compared to Atherogenic indices.

Table 4. ROC curve analysis using atherosclerosis markers to distinguish the different groups in Control and AS group.

	Area	**Std. Error**	**P-value**	**95% CI**	
				Lower Bound	**Upper Bound**
G-score	1.000	.000	<0.0001****	1.000	1.000
miR-125b	.863	.074	<0.01 **	.724	1.000
TYG	.680	.105	.138	.475	.885
AIP	.699	.102	.100	.498	.900
CRI-I	.484	.114	.893	.259	.708
CRI-II	.598	.114	.419	.375	.821

Note: * $p <0.05$, ** $p <0.01$, *** $p <0.001$. TYG: triglyceride glucose index; AIP: Atherogenic index of plasma; CRI-I: Castelli's Risk Index I; CRI-II: Castelli's Risk Index II.

Resistin and *miR-20a-5p* levels in PBMCs and risk factor for AS

By using a logistic regression analysis, we further assessed the relationships between gene expression levels and the presence of AS. The investigation proved that a significant reduction in *miR-20a* is a new risk factor and is linked with the presence of AS ($p <0.05$). The odds ratio of *miR-20a* was 0.65 (95% CI, 0.44–0.92), and is illustrated in Table 5. However, the results from logistic regression analysis for atherosclerosis did not show a significant difference for the expression of *Resistin* ($p =0.07$). The odds ratio of *Resistin* was 1.057 (95% CI, 0.99–1.23).

PBMC *miR-20a-5p*, *miR-125b-5p*, *miR-124-3p* correlation with, *Resistin, CD36, TNF-α, TLR4,* FBS and Atherogenic indices

The correlations between genes were further analyzed in the PBMC. miR-124 had a positive correlation with Resistin (Figure. 5, A: r = -0.34, p <0.01). Resistin had a positive correlation with *CD36* and *TNF-α* (Figure. 5, B: r = 0.37, $p< 0.01$), (Figure 5, C: r = 0.4, $p< 0.01$), respectively. In addition, the relationship between *TNF-α* and *TLR4* (Figure. 5, D: r = 0.46, $p <0.001$) was significantly positive. The correlation between TLR4 and miR-20a was not significant (r = 0.23, $p = 0.42$).

Based on Table 6, The correlation of gene expression levels (*miR-125b*, *miR-20a*, *TNF-α,* and *TLR4*) and various indices analyzed to understand potential associations in atherosclerotic patients. *miR-20a* has a negative and significant relationship with FBS (r = -0.3, $p < 0.05$) and TYG (r = -0.35, $p < 0.05$), also miR-124 inversely correlated with FBS (r= -0.24, $p < 0.05$). Key findings showed a positive correlation between *miR-125b* and the G-score (r = 0.337, $p < 0.01$), a negative correlation between *miR-20a* and the G-score (r = -0.331, $p < 0.05$), and a significant positive correlation between *TLR4* and the G-score (r = 0.256, $p < 0.05$). The study found a positive correlation between *TNF-α* levels with the number of involved vessels (r = 0.366, $p < 0.05$).

Table 5. Evaluation of atherosclerosis with Four variables such as *miR-20a*, *miR-125b*, *TLR4* and *TNF-α* expression levels by controlling confounding variables of age, sex, history of hypertension, smoking, and BMI using logistic regression.

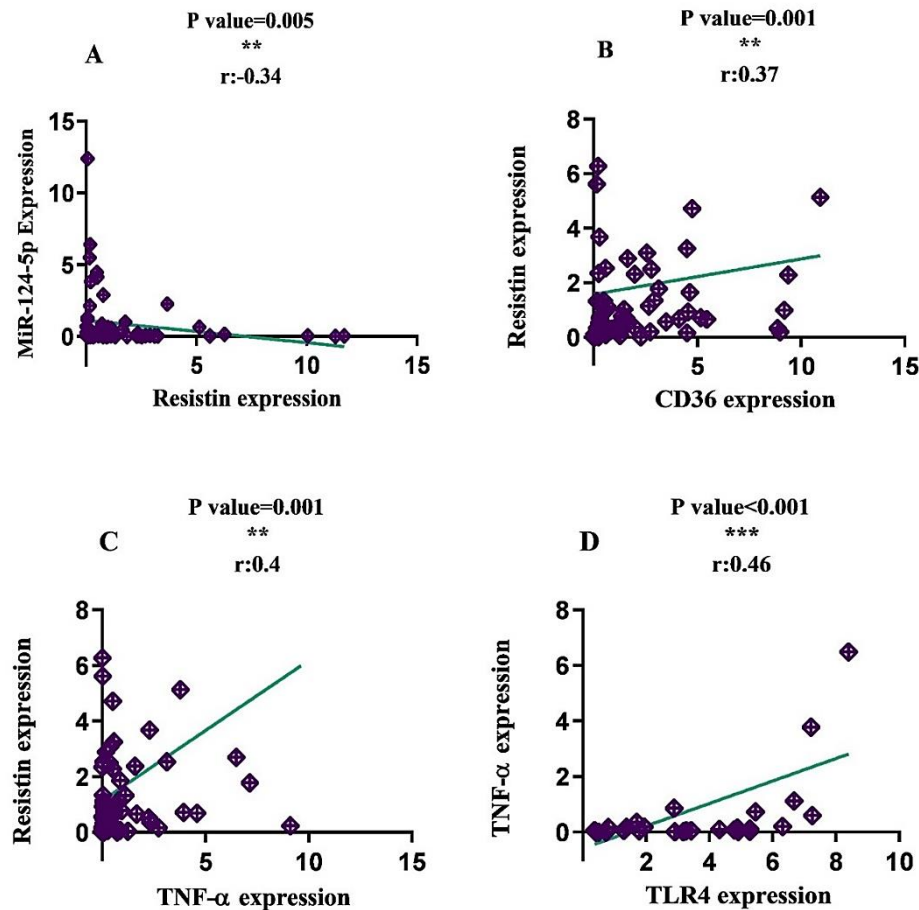| **Variable**	**Odd ratio**	**CI 95%**	**P-value**
miR-20a	0.65	(0.44-0.92)	<0.05*
miR-125b	1.034	(0.98-1.08)	0.218
TLR4	2.50	(0.065-6.57)	0.062
TNF-α	1.027	(0.97-1.08)	0.35

Note: * $p <0.05$, ** $p <0.01$, *** $p <0.001$.

Figure 5. Correlation analysis for *miR-124, Resistin, CD36, TNF-α, TLR4*. Correlation of *miR-124* and *Resistin* (r = -0.34) (A); Correlation of *Resistin* and *CD36* (r = -0.39) (B); Correlation of *Resistin* and *TNF-α* (r = 0.4) (C); Correlation of *TNF-α* and *TLR4* (r = 0.46) (D). Note: FBS: Fasting Blood Sugar; AIP: Atherogenic index of plasma; TYG: Triglyceride Glucose. (*p < 0.05, **p < 0.01, ***p<0.001)."

Table 6. Correlation analysis for gene level, miRNA expression and Atherogenic indices.

Variable	Spearman	FBS	TG	CL	HDL	LDL	AIP	TYG	CRI-I	CRI-II	Involved vessels	Gensini score
miR-125b	r	0.036	0.206	-0.062	-0.145	0.017	0.421	0.168	0.030	0.182	0.119	0.337
	p-value	0.767	0.209	0.710	0.421	0.922	<0.05*	0.313	0.871	0.304	0.315	<0.01**
miR-20a	r	-0.319	-0.210	-0.217	-0.214	-0.155	0.049	-0.352	-0.164	0.017	-0.215	-0.331
	p-value	<0.05*	0.234	0.218	0.247	0.407	0.805	<0.05*	0.396	0.928	0.08	<0.05*
miR-124	r	-0.246	S0.018	0.226	-0.046	0.016	0.101	-0.053	0.041	0.264	0.142	-0.19
	p-value	<0.05*	0.909	0.17	0.78	0.383	0.553	0.373	0.357	0.108	0.390	0.130
Resistin	r	0.053	-0.02	0.121	0.108	0.170	-0.021	-0.087	0.188	0.110	0.198	0.141
	p-value	0.668	0.903	0.458	0.532	0.307	0.902	0.595	0.271	0.511	0.233	0.264
CD36	r	-0.041	0.138	0.180	-0.020	-0.044	-0.039	0.141	0.118	0.087	0.061	0.003
	p-value	0.839	0.395	0.273	0.908	0.800	0.826	0.391	0.505	0.613	0.630	0.985
TLR4	r	0.089	0.335	0.195	0.211	0.156	0.331	0.223	0.150	0.119	0.114	0.256
	p-value	0.626	0.148	0.424	0.400	0.523	0.155	0.346	0.567	0.627	0.260	<0.05*
TNF-α	r	-0.045	0.019	0.077	-0.002	-0.007	0.150	0.110	-0.001	-0.039	0.366	0.140
	p-value	0.918	0.912	0.649	0.992	0.966	0.398	0.516	0.998	0.822	<0.05*	0.279

Note: * *p* <0.05, ** *p* <0.01, *** *p* <0.001. TYG: triglyceride glucose index; AIP: Atherogenic index of plasma; CRI-I: Castelli's Risk Index I; CRI-II: Castelli's Risk Index II.

Relationship Between AS *miR-20a* and AS-Associated Biological Signaling Pathways, In Silico

We used the miR-Target Scan database (https://www.microrna-target.org/) and the Kegg pathway (https://www.genome.jp/kegg/pathway.html) to link the biological function of *miR-20a, miR-124* and calcification-related signaling to better understand the AS biology of this miR expressed in PBMCs.

Primary interactions between the target mRNA and *hsa-miR-20a-5p* (UAAAGUGCUUAUAGUGCAGGUAG) and *has-miR-124-3p* (UAAGGCACGCGGUGAAUGCCAA) were identified using the RNA-hybrid program (https://bibiserv.cebitec.uni-bielefeld.de/rnahybrid/)

(Figure. 6). The minimum free energy (mfe) value indicates the stability of the miRNA-mRNA duplex, with more negative values (e.g., -25.8 kcal/mol for *miR-124* and *Resistin*) representing higher predicted binding affinity and stability. Generally, the findings indicated that levels of *TLR4* expression increased in PBMCs of patients with AS, resulting in increased expression of *miR-125b* and reduced expression of *miR-20a*, and subsequently AS progression. Furthermore, a decrease in levels of *miR-124* may lead to an increase in levels of Resistin, indicating a negative correction. Resistin in turn, had a positive correlation with both *CD36* and *TNF-α* (Figure. 7).
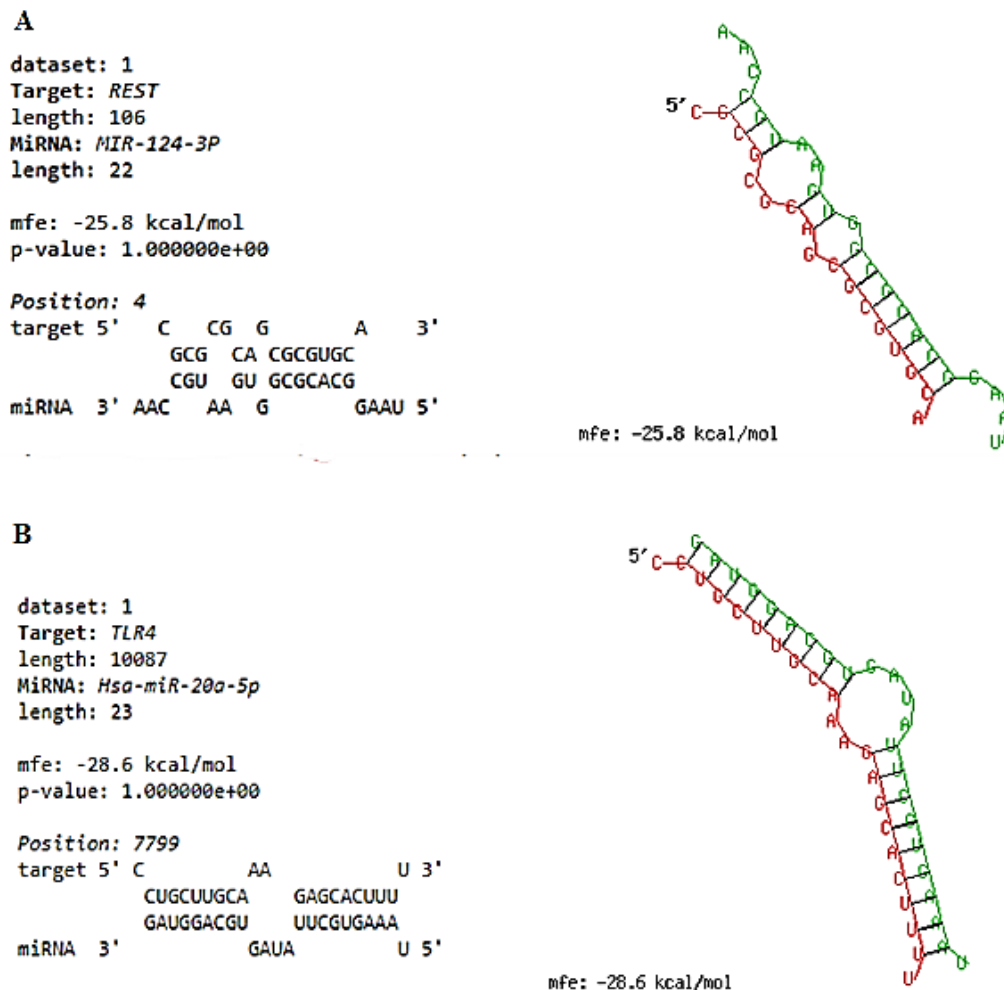

Figure 6. Prediction of post-transcriptional interaction between *Resistin* (A) and *TLR4* (B) mRNA 3'UTR with *miR-124* and *miR-20a* assessed by RNA-Hybrid program. The interaction produced a significant minimum free energy (−25.8 mfe for Resistin and −28.6 mfe for *TLR4*) forming a stable hybrid structure. The minimum free energy (mfe) value indicates the stability of the miRNA-mRNA duplex, with more negative values (e.g., -25.8 kcal/mol) representing higher predicted binding affinity and stability.
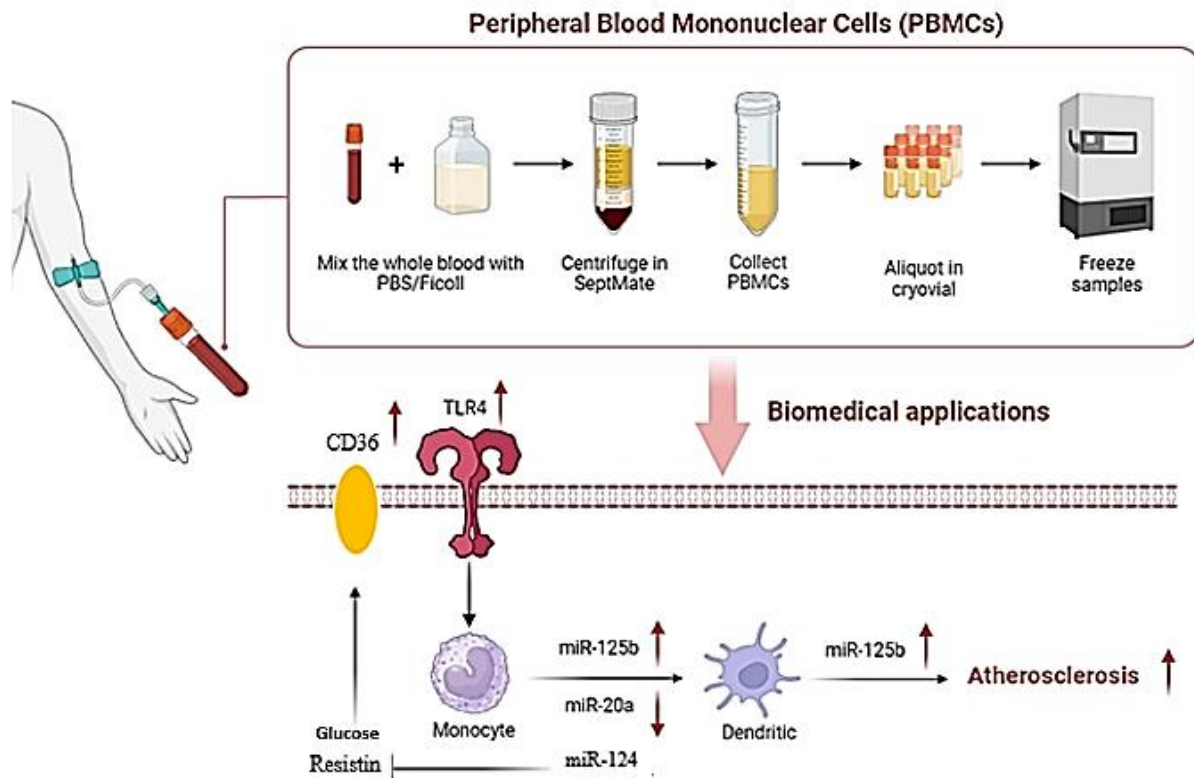
Figure 7. A proposed integrative model of miRNA–mRNA crosstalk in the pathogenesis of atherosclerosis.
This schematic summarizes a hypothesized mechanistic network derived from expression and correlation analyses in PBMCs from atherosclerosis patients. Key observations include: A) Downregulation of *miR-20a-5p*, which may promote *TLR4*-mediated activation of NF-κB and *TNF-α* secretion, particularly under hyperglycemic conditions. B) Reduced *miR-124-3p* expression, potentially enabling upregulation of *Resistin*, which correlates positively with *CD36* and *TNF-α*. C) *Resistin* may further amplify inflammatory signaling via *TLR4* and enhance *CD36*-dependent ox-LDL uptake, contributing to foam cell formation. D) Upregulation of *miR-125b-5p*, identified here as a potential biomarker, may modulate lipid metabolism and inflammatory pathways. Solid lines denote interactions supported by significant correlation data in this study and prior functional evidence; dashed lines indicate proposed interactions based largely on established literature. This model offers a testable framework for future mechanistic investigation into miRNA-mediated regulation of inflammatory and metabolic processes in atherosclerosis.

Discussion

The initiation, progression, and diagnosis of coronary artery disease can be linked to the participation of miRNAs in a variety of cellular physiological processes associated with atherosclerosis, particularly those regulating lipid and carbohydrate homeostasis. PBMCs are a desirable basis for biological experiments due to their direct availability and preparation of peripheral blood. Moreover, the physiological and molecular mechanisms of these cells and the underlying inflammation appear to play a crucial pathogenic role in the pathogenesis of heart disease (30). Based on our understanding, this is the first report proving that low expression of *miR-20a* in PBMCs appears to be a risk factor for patients with AS. Also, we found that *miR-*

125b could serve as a non-invasive biomarker for the diagnosis of AS while miR-125b shows potential as a biomarker for AS, further validation is necessary due to its limited sensitivity. The PBMC-*miR-20a* level in AS patients was significantly lower than that of healthy subjects. However, the expression of *Resistin* and *TLR4* in PBMC was elevated in AS patients. The correlation between these microRNAs and serum glucose concentrations, atherogenic indices, lipid profiles, and inflammatory mediators (*TNF-α* and *TLR4*) was evaluated. *miR-20a* and *miR-124* show a positive correlation with fasting blood glucose. The study suggests that *miR-124* may be associated with *Resistin*, a gene that is positively correlated with *CD36* and *TNF-α*. This indicates a new mechanism in the progression of atherosclerosis involving this signaling pathway.

In this research, we revealed that *miR-20a* PBMCs were reduced and serum FBS and TG increased more in the control group than in the AS group. *miR-20a* correlated negatively with the FBS and TYG indexes. The TYG index was calculated as a formula based on FBS and TG. The TYG index was initially investigated as a high-sensitivity and specificity marker for the detection of insulin resistance. It was later found that type 2 diabetes and metabolic syndrome, which increase the risk of cardiometabolic disease, are predicted by the TYG index (31). To satisfy the body's need for energy, hyperglycemia causes changes in lipid metabolism. The progression of vascular complications is influenced by endothelial cell dysfunction resulting from hyperlipidemia (32). Therefore, based on our study, it was found that *miR-20a* reduction increases the risk of atherosclerosis almost twofold, which may be related to PBMC-induced inflammatory target genes. Additionally, the inverse correlation with the G-score implies that heightened *miR-20a* levels might mitigate the severity of CAD, presenting a promising avenue for therapeutic exploration.

TLR4 associated with inflammatory pathway-based atherosclerosis progression, were identified as targets according to the hybrid RNA program, with a high score for *Has-miR-20a-5*. *TLR4*, a sentinel of the immune system, emerges as a key player in CAD severity. Nevertheless, our study did not reveal a statistically significant association between miR-20a and TLR4. This suggests the possibility that an alternative, more critical target might be instrumental in influencing clinical outcomes. The positive correlation with the G-score implicates *TLR4* in orchestrating immune responses that contribute to the progression of atherosclerotic lesions. This connection invites further exploration into the immunomodulatory aspects of atherosclerosis and the potential therapeutic implications of *TLR4* modulation. The G-score serves as a standardized measure to assess the severity of coronary artery lesions, considering both the degree of stenosis and the number of vessels affected for detection. The positive correlation with the number of involved vessels suggests *TNF-α*'s role in orchestrating a systemic impact, influencing the extent of atherosclerotic lesions across coronary vessels.

The current study suggests a possible link between the downregulation of *miR-20a* and heart damage associated with ischemia. An *in vitro* experiment revealed that exposure to oxidized LDL particles suppressed the *miR-20a* gene in human aortic endothelial cells. *MiR-20a* upregulation prevented the generation of ROS in cells, reduced inflammatory conditions, and slowed the progression of atherosclerosis (13). In addition, transfected *miR-20a* supports myocardial cell line survival and diminishes apoptosis, preventing ischemia/reperfusion injury (33). *Phosphatase and tensin homolog* (*PTEN*) were specifically targeted through *miR-20a* to promote venous endothelial cell survival and proliferation (34).

Moreover, based on an animal study, *miR-20a* mimics reduced blood glucose levels. It improved lipid profiles in the control group compared to a group of diabetic rats (using *miR-20a* mimic in rats with STZ-induced diabetes) (35). The levels of *NF-κB* and *TLR-4* mRNA in aortic tissue were higher in the diabetes group than in the control group and the *miR-20a* mimic group (36). The significant inverse correlations between miR-20a and both FBS and the TYG index are particularly intriguing. The TYG index is a well-established surrogate marker of insulin resistance. This finding suggests a potential novel role for *miR-20a* in regulating systemic glucose metabolism and insulin signaling, possibly within immune cells themselves, which could subsequently influence their inflammatory activation state and contribute to atherogenesis. This hypothesis is supported by experimental evidence showing that manipulation of *miR-20a* levels can influence glycemic control in diabetic models. This aligns with animal studies showing miR-20a mimic administration improves glycemic control.

The current results stated that *miR-125b* is a more useful biomarker for detecting atherosclerosis than TYG and AIP indexes. The positive correlation discovered between *miR-125b* and the Gensini score underscores its potential role as a regulatory molecule in CAD severity. Higher *miR-125b* levels may act as a biomarker for more extensive atherosclerotic lesions, prompting further exploration of its intricate involvement in disease progression. We hypothesized that *miR-125b* may play a major part in the onset of atherosclerosis.

Consistent with the outcomes of this study, 26 patients and 25 healthy controls were analyzed for *miR-125b* by the Pelin Telkoparan-Akillilar et al study. This finding shows that *miR-125b*, which targets *NRF2*, can be utilized as a new indicator to detect atherosclerosis (37). The Kegang Jia's study found that in acute

coronary syndrome patients, the *miR-125b* positive group had a lower cumulative survival rate after acute myocardial infarction than the negative group (38). Isabel Moscoso et al. discovered that *miR-125a* downregulation was connected to a significant improvement in left ventricular ejection fraction in the follow-up of patients undergoing cardiac resynchronization therapy (39). Based on Varun Nagpal et al. research, *miR-125b* is crucial for the induction of cardiac fibrosis and functions as a powerful repressor of a variety of antifibrotic pathways. Innovative treatment approaches incorporating the suppression of *miR-125b* can be used to treat human heart fibrosis and other fibrotic disorders (40). In contrast to the current study, Ahmad SB et al. demonstrated that abnormalities in cardiac structure and function were caused by the loss of miR-125b function in mouse hearts following acute myocardial infarction (41). It is debatable how *miR-125b* affects cardiovascular disorders. *MiR-125b* emerges as a promising non-invasive biomarker for diagnosing AS, given its positive correlation with the Gensini score, which reflects the extent of coronary lesions. The varied expression of *miR-125b* in different cardiovascular conditions, as reported in previous studies, indicates its complex role in disease progression and highlights the need for further research to unravel its precise mechanisms.

In this study, the expression levels of *miR-124, Resistin*, and *CD36* genes differed between the two control and AS groups. While *miR-124* and *CD36* did not show statistical significance, *Resistin* exhibited a significant increase in the AS group and showed a positive correlation with *miR-124*. Multiple studies have been dedicated to evaluating the roles of *miR-124, Resistin* and *CD36* in atherosclerosis. According to Liang et al., *miR-124* levels dropped in ApoE−/− animal models and atherosclerosis patients, lowering cytokines and preventing macrophage death by regulating p38. This suggests that upregulation of *miR-124* could be a viable therapeutic strategy (42). In our research, *miR-124* was positively correlated with fasting blood glucose and *Resistin*. Yanhui He's research indicates that while *miR-124* was downregulated in human retinal microvascular endothelial cells (HRMECs) triggered by high glucose (HG), overexpression decreased the cellular damage caused by HG. *miR-124* alleviated cell injury by modulating the p38MAPK signaling pathway (43). Mohammadzadeh GH et al. found that high

Resistin expression in PBMCs of diabetic nephropathy patients is associated with *TNF-α* and *miR-124* expressions (18).

Resistin is involved in human health by binding to receptors like *TLR4*, leading to vascular inflammation, lipid accumulation, and plaque instability. It affects endothelial cells, vascular smooth muscle cells, and macrophages, causing cardiovascular damage (44). Based on Min Luo examinations, *Resistin* increases *CD36* expression at both mRNA and protein levels, without affecting the class A macrophage scavenger receptor. This suggests *Resistin* promotes lipid accumulation in macrophages and may modulate macrophage-to-foam cell transformation. The current research showed that *Resistin* and *CD36* were directly correlated (45). The current study also identifies the significant upregulation of *Resistin* and *TLR4* in AS patients, linking these factors to the inflammatory pathways that exacerbate atherosclerosis. The interplay between *miR-124*, *Resistin*, and *CD36* further supports the multifaceted involvement of these molecules in lipid metabolism and inflammatory responses (46), suggesting potential therapeutic targets for managing cardiovascular disease.

The lack of a significant difference in *miR-124* expression between our AS and control groups contrasts with some previous studies conducted on vascular tissues or animal models. This discrepancy could be attributed to several factors: The heterogeneity of PBMCs: *miR-124* expression might be altered in specific immune cell subpopulations (e.g., monocytes versus lymphocytes), and changes could be diluted when analyzing total PBMCs. The stage of atherosclerosis: Our patient cohort might represent a disease stage where *miR-124* dysregulation in circulation is not yet pronounced. (3) Medication effects: Concomitant medication, particularly statins, may modulate *miR-124* expression and mask inherent differences. Compartmentalization: miR-124's role might be more tissue-specific, with significant changes occurring locally within the atherosclerotic plaque rather than in circulating cells. Future studies involving PBMC subset sorting or analysis of plasma-derived exosomes could provide further clarity.

The study on atherosclerosis biomarkers has limitations due to the small sample size of 45 healthy people and 45 atherosclerosis patients and the use of miRNA-based diagnostics. Furthermore, while a post-hoc analysis indicated sufficient power for our primary

findings, the sample size was relatively modest for a biomarker discovery study. The cross-sectional design and single center for sample collection limit causal linkages, providing only a snapshot of miRNA and gene expression levels. Future research should focus on larger, more diverse populations and use animals and cell lines to expand on the findings. Furthermore, we found that *miR-125b* could serve as a potential non-invasive biomarker for the diagnosis of AS, though its modest sensitivity (52%) indicates it may be more useful as part of a panel rather than a standalone test and requires validation in larger, independent cohorts. Another limitation, the observational nature of our study and the lack of functional experiments (e.g., gain-of-function or loss-of-function studies in cells) mean that we cannot establish causal relationships between the observed miRNA and gene expression changes.

As a result of this study, reduced levels of *miR-20a* in PBMCs of patients were significantly correlated with the progression of AS. On the other hand, research indicates that *miR-125b* may serve as a potential biomarker for the identification of AS. However, *miR-124, CD36*, and *TNF-α* expression levels showed no significant differences between groups, indicating the need for further research on these genes and their relationship with AS. Increased *TLR4* and *Resistin* levels, as well as the correlations between *miR-124, Resistin, CD36*, and *TNF-α*, point to a new mechanism in the development of AS. Interestingly, *miR-20a* and *miR-124* showed negative relationships with fasting blood glucose, suggesting that these reduced miRNA levels are linked to high blood glucose levels. It is crucial to note that these correlations are associative and do not establish causality; future mechanistic studies in cell cultures or animal models are required to validate this proposed pathway.

These findings suggest potential roles for some miRs in lipid metabolism, glucose regulation, and inflammation in the context of atherosclerosis. The highlighted correlations provide significant new insights into the interplay between gene expression and clinical features in atherosclerosis. Nonetheless, we recommend conducting clinical trials to mechanistically elucidate the associations of these miRNAs and their targets in AS and other cardiovascular diseases, particularly focusing on the overexpression of *miR-20a-5p* for atherosclerosis treatment. To our knowledge, no previous research has examined *miR-20a* levels in atherosclerosis patients;

prior studies have focused solely on cells or animal models. This finding could serve as a crucial point for further investigations into *miR-20a* and its potential role in treating atherosclerosis.

Acknowledgements

Funding

References

1. Soehnlein O, Libby P. Targeting inflammation in atherosclerosis—from experimental insights to the clinic. Nat. Rev. Drug Discov. 2021;20(8):589-610.

2. Milutinović A, Šuput D, Zorc-Pleskovič R. Pathogenesis of atherosclerosis in the tunica intima, media, and adventitia of coronary arteries: An updated review. BJBMS. 2020;20(1):21.

3. Achim A, Péter OÁ, Cocoi M, et al. Correlation between Coronary Artery Disease with Other Arterial Systems: Similar, Albeit Separate, Underlying Pathophysiologic Mechanisms. J. Cardiovasc. Dev. Dis. 2023;10(5):210.

4. Rafieian-Kopaei M, Setorki M, Doudi M, et al. Atherosclerosis: process, indicators, risk factors and new hopes. Int. J. Prev. Med. 2014;5(8):927.

5. Radke D, Jia W, Sharma D, et al. Tissue engineering at the blood-contacting surface: A review of challenges and strategies in vascular graft development. Adv. Healthc. Mater. 2018;7(15):1701461.

6. Si Y, Tian H, Dong B, et al. Effects of hydrogen as adjuvant treatment for unstable angina. Exp. Biol. Med. 2021;246(18):1981-9.

7. Andreadi A, Bellia A, Di Daniele N, et al. The molecular link between oxidative stress, insulin resistance, and type 2 diabetes: A target for new therapies against cardiovascular diseases. Curr. Opin. Pharmacol. 2022;62:85-96.

8. Martin P, Gurevich DB, editors. Macrophage regulation of angiogenesis in health and disease. Semin Cell Dev Biol.; 2021: Elsevier.

9. Soloperto G, Casciaro S. Progress in atherosclerotic plaque imaging. World J. Radiol. 2012;4(8):353.

10. O'Brien J, Hayder H, Zayed Y, et al. Overview of microRNA biogenesis, mechanisms of actions, and circulation. Front. Genet. 2018;9:402.

11. Mestdagh P, Boström A-K, Impens F, et al. The miR-17-92 microRNA cluster regulates multiple components of the TGF-β pathway in neuroblastoma. Mol cell. 2010;40(5):762-73.

12. Arzhanov I, Sintakova K, Romanyuk N. The role of miR-20 in Health and disease of the central nervous system. Cells. 2022;11(9):1525.

13. Chen M, Li W, Zhang Y, et al. MicroRNA-20a protects human aortic endothelial cells from Ox-LDL-induced inflammation through targeting TLR4 and TXNIP signaling. Biomed. Pharmacother. 2018;103:191-7.

14. Liang Y-P, Liu Q, Xu G-H, et al. The lncRNA ROR/miR-124-3p/TRAF6 axis regulated the ischaemia reperfusion injury-induced inflammatory response in human cardiac myocytes. J. Bioenerg. Biomembr. 2019;51:381-92.

15. Ghafouri-Fard S, Shoorei H, Bahroudi Z, et al. An update on the role of miR-124 in the pathogenesis of human disorders. Biomed. Pharmacother. 2021;135:111198.

16. Azizoğlu M, Ayaz L, Bayrak G, et al. Evaluation of miRNAs related with nuclear factor kappa B pathway in lipopolysaccharide induced acute respiratory distress syndrome. Int. J. Mol. Med. 2020;9(2):130.

17. Choe N, Kwon DH, Shin S, et al. The micro RNA miR-124 inhibits vascular smooth muscle cell proliferation by targeting S100 calcium-binding protein A4 (S100A4). FEBS Lett. 2017;591(7):1041-52.

18. Monjezi A, Khedri A, Zakerkish M, et al. Resistin, TNF-α, and microRNA 124-3p expressions in peripheral blood mononuclear cells are associated with diabetic nephropathy. Int. J. Diabetes Dev. Ctries. 2022:1-8.

19. Pang L, Li X-l. Mechanism of resistin-induced enhancement of proliferation and migration of ovarian cancer cells. Arch Med Sci. 2020;16(1):1-9.

20. Acquarone E, Monacelli F, Borghi R, et al. Resistin: A reappraisal. Mechanisms ageing dev. 2019;178:46-63.

21. Ghaemmaghami S, Mohaddes SM, Hedayati M, et al. Resistin and visfatin expression in HCT-116 colorectal cancer cell line. Int. J. Mol. Med. 2013;2(3):143.

22. Zhao L, Varghese Z, Moorhead J, et al. CD36 and lipid metabolism in the evolution of atherosclerosis. Br. Med. Bull. 2018;126(1):101-12.

23. Mellal K, Omri S, Mulumba M, et al. Immunometabolic modulation of retinal inflammation by CD36 ligand. Sci. Rep. 2019;9(1):12903.

24. Mosavi E, Bandehpour M, Mostafazadeh A, et al. Plasma TNF-α elevation in biologic naive rheumatoid arthritis patients belonging to a population with new mutations in TLR4 and CYP51A1 genes without association with disease-related antibodies levels. Int. J. Mol. Med. 2024;13(2):171.

25. Gómez-Bañuelos E, Martín-Márquez BT, Martínez-García EA, et al. Low levels of CD36 in peripheral blood monocytes in subclinical atherosclerosis in rheumatoid arthritis: a cross-sectional study in a Mexican population. Biomed Res. Int. 2014;2014(1):736786.

26. Hueso M, Griñán R, Mallen A, et al. MiR-125b downregulates macrophage scavenger receptor type B1 and reverse cholesterol transport. Biomed. Pharmacother. 2022;146:112596.

27. Piergentili R, Gullo G, Cucinella G, et al. miR125-Centered ceRNETs in Breast Cancer. Clinical, Molecular and Ethical Aspects in Personalized Medicine. Non-Coding RNA. 2025;11(4):50.

28. Chao CT, Yeh HY, Yuan TH, et al. MicroRNA-125b in vascular diseases: An updated systematic review of pathogenetic implications and clinical applications. J Cell Mol Med. 2019;23(9):5884-94.

29. Mirderikvand A, Shahsavari G, Moayyed Kazemi A, et al. Exploring the Role of MicroRNA-125b, signal transducer and activator of transcription 3 (STAT3) and sirtuin 6 (SIRT6) Genes in Blood Leukocytes of Atherosclerosis Patients and Their Correlations with Biochemical Parameters; A Case-Control Study. Rep Biochem Mol Biol. . 2024;12(4):631-42.

30. Voellenkle C, Van Rooij J, Cappuzzello C, et al. MicroRNA signatures in peripheral blood mononuclear cells of chronic heart failure patients. Physiol. Genomics. 2010;42(3):420-6.

31. Jin J-L, Cao Y-X, Wu L-G, et al. Triglyceride glucose index for predicting cardiovascular outcomes in patients with coronary artery disease. J. Thorac. Dis. 2018;10(11):6137.

32. Sena CM, Pereira AM, Seiça R. Endothelial dysfunction—a major mediator of diabetic vascular disease. Biochim. Biophys. Acta, Mol. Basis Dis. 2013;1832(12):2216-31.

33. Gong X-Y, Zhang Y. Protective effect of miR-20a against hypoxia/reoxygenation treatment on cardiomyocytes cell viability and cell apoptosis by targeting TLR4 and inhibiting p38 MAPK/JNK signaling. In Vitro Cell. Dev. Biol. Anim. 2019;55:793-800.

34. Wang D, Wang Y, Ma J, et al. MicroRNA-20a participates in the aerobic exercise-based prevention of coronary artery disease by targeting PTEN. Biomed. Pharmacother. 2017;95:756-63.

35. Li Y, Zheng L, Li Y-H, et al. MiR-20a ameliorates diabetic angiopathy in streptozotocin-induced diabetic rats by regulating intracellular antioxidant enzymes and VEGF. Eur. Rev. Med. Pharmacol. Sci. 2020;24(4).

36. Li Y, Zheng L, Li Y, et al. MiR-20a ameliorates diabetic angiopathy in streptozotocin-induced diabetic rats by regulating intracellular antioxidant enzymes and VEGF. Eur. Rev. Med. Pharmacol. Sci. 2020;24:1948-55.

37. Telkoparan-Akillilar P, Cevik D, Yilmaz A. Expression patterns of miR-34a, miR-125b, miR-221 and antioxidant gene NRF2 in plasma samples of patients with atherosclerosis. J. Biosci. 2022;47(1):1.

38. Jia K, Shi P, Han X, et al. Diagnostic value of miR-30d-5p and miR-125b-5p in acute myocardial infarction. Mol med rep. 2016;14(1):184-94.

39. Moscoso I, Cebro-Márquez M, Martínez-Gómez Á, et al. Circulating miR-499a and miR-125b as Potential Predictors of Left Ventricular Ejection Fraction Improvement after Cardiac Resynchronization Therapy. Cells. 2022;11(2):271.

40. Nagpal V, Rai R, Place AT, et al. MiR-125b is critical for fibroblast-to-myofibroblast transition and cardiac fibrosis. Circulation. 2016;133(3):291-301.

41. Bayoumi AS, Park K-m, Wang Y, et al. A carvedilol-responsive microRNA, miR-125b-5p protects the heart from acute myocardial infarction by repressing pro-apoptotic bak1 and klf13 in cardiomyocytes. J Cell Mol Med. 2018;114:72-82.

42. Liang X, Wang L, Wang M, et al. MicroRNA-124 inhibits macrophage cell apoptosis via targeting p38/MAPK signaling pathway in atherosclerosis development. Aging (Albany NY). 2020;12(13):13005.

43. Zhao H, He Y. MiR-124-3p suppresses the dysfunction of high glucose-stimulated endothelial cells by targeting G3BP2. Front. Genet. 2021;12:723625.

44. Tarkowski A, Bjersing J, Shestakov A, et al. Resistin competes with lipopolysaccharide for binding to toll-like receptor 4. J Cell Mol Med. 2010;14(6b):1419-31.

45. Xu W, Yu L, Zhou W, et al. Resistin increases lipid accumulation and CD36 expression in human macrophages. Biochem. Biophys. Res. Commun. 2006;351(2):376-82.

46. Pezeshki SP, Darabi MK, Nazeri Z, et al. Mesenchymal stem cells therapy led to the improvement of spatial memory in rats with alzheimer's disease through changing the expression of LncRNA TUSC7/miR-449a/PPARγ and CD36 genes in the brain tissue. Int. J. Mol. Med. 2023;12(2):108.